Cellular Oncology 28 (2006) 177–190
IOS Press

Hepatitis C virus core protein transforms murine fibroblasts by promoting genomic instability

Irina S. Smirnova [a], Nikolai D. Aksenov [a], Elena V. Kashuba [c], Pawan Payakurel [c], Vadim V. Grabovetsky [d,e], Alexei D. Zaberezhny [d,e], Maxim S. Vonsky [a], Lubov Buchinska [f], Peter Biberfeld [c], Jorma Hinkula [b,c] and Maria G. Isaguliants [b,d,*]

[a] *Institute of Cytology RAS, St. Petersburg, Russia*
[b] *Swedish Institute for Infectious Disease Control, Stockholm, Sweden*
[c] *Microbiology and Tumor Biology Center (MTC) and Department of Immunopathology, Karolinska Institute, Stockholm, Sweden*
[d] *Ivanovsky Institute of Virology, Moscow, Russia*
[e] *Narvac R&D Company, Moscow, Russia*
[f] *R.E. Kavetsky Institute of Experimental Pathology, Oncology and Radiobiology, National Academy of Sciences of Ukraine, Kiev, Ukraine*

Abstract. The oncogenic potential of hepatitis C virus (HCV) core protein has been demonstrated, but the precise mechanism of cell transformation triggered by HCV core is still unclear. This study shows that constitutive expression of HCV core protein (core) in NIH 3T3 murine fibroblasts triggers malignant transformation. At the preneoplastic stage, clones that expressed HCV core constitutively demonstrated genomic instability seen as disruption of the mitotic spindle cell checkpoint leading to increased ploidy. Transformation was completed by the loss of DNA and resistance to apoptosis induced by serum starvation. Simultaneously, cells acquired a capacity for anchorage independent growth and absence of contact inhibition. Inoculation of these transformed cells into severe combined immune deficiency (SCID) mice led to formation of solid core-expressing tumors. Transformation and tumorigenicity of core-expressing cell lines coincided with a 5- to 10-fold repression of endogenous p53 transactivation. Thus, long-term HCV core expression alone is sufficient for complete transformation of immortal fibroblasts that can then induce tumors in a susceptible host. This data suggests that malignant transformation by HCV core may occur through primary stress, induction of genomic instability, and further HCV core-induced rescue of surviving mutated cells.

Keywords: Hepatitis C virus, core protein, constitutive expression, fibroblast, mitotic spindle cell checkpoint, genomic instability, malignant transformation, p53, fibrosarcoma

1. Introduction

Hepatitis C virus (HCV) is a positive strand RNA virus that belongs to the Hepaciviridae genus within the Flaviviridae family. HCV infection has a wide spectrum of clinical presentations; 55% to 85% of patients do not clear virus, but develop chronic hepatitis C [14]. The chronic sequelae of hepatitis C include progressive hepatic fibrosis and cirrhosis, the major risk factors of hepatocellular carcinoma (HCC), and eventually HCC [17]. It is becoming increasingly evident that HCV not only causes cell renewal coupled with inflammation that indirectly triggers HCC, but is directly involved in hepatocarcinogenesis [17,27,49]. One of the suspected inducers of HCV-related HCC is the nucleocapsid (core) protein [27]. It has versatile effects on the host cells by direct/indirect regulation of various promoters and modulation of apoptosis [27,58]. By transmitting growth stimuli and interfering with intracellular signal transduction, HCV core can immortalize, and in collaboration with onco-

*Corresponding author: Maria G. Isaguliants, Swedish Institute for Infectious Disease Control, Nobels v 18, 171 82 Solna, Sweden. Tel.: +46 8 4572609; Fax: +46 8 337272; E-mail: maria.isaguliants@smi.ki.se.

genes, transform mammalian cells [46]. *In vivo*, progression to tumors is often driven by growth constraint of the host tissue associated with stress conditions [30]. Transiently expressed HCV core exerts a multitude of stresses, such as an oxidative stress with mitochondrial injury [31,37,41], and NF-kappa B activation-dependent endoplasmic reticulum (ER) stress mediated by the ER-overload [24]. As an *in vivo* implication, mice transgenic for HCV core gene often develop malignant lymphomas, hepatocellular carcinomas and adenomas [20,27].

Part of the oncogenic potential HCV core protein gains through affecting activities of the tumor suppressor protein TP53 (p53). In transiently transfected cells, HCV core augments p53 DNA-binding and transactivation. This leads to the cell growth arrest at the G1 phase of the cell cycle or induction of apoptosis [33, 42]. Indirect p53 activation through core-induced up-regulation of cellular proto-oncogenes [44] could also play a role. Besides, HCV core modulates the activity of p53 transcriptional targets, such as cyclin kinase inhibitor p21 [29,33,39,62]. An increase in p21 expression acts as a stress factor by decreasing percentage of cells in the S-phase along with accumulation of cells in the G0/G1 phase [39].

Controversial data exist on the effects of HCV core in the constitutively expressing cell lines. The activity of p53 and the transcriptional targets of p53, p21 and the 14-3-3 family, appears to be suppressed [1,29, 46,62]. In addition, core expression ($\geqslant$72 h) induces up-regulation of cyclins E1 and D1 [6,64], decreases the Rb levels and up-regulates E2F-1, disrupting the performance of the pRB-E2F-1 complex as transcriptional repressor [7]. These HCV core activities allow for p53-uncontrolled rapid cell proliferation. Unlimited cell growth is further promoted by HCV core binding to the intracellular signal-transducing portion of death receptors that displaces signalling molecules and interferes with apoptosis [28,58]. Thus, HCV core effects eukaryotic cells in a biphasic fashion, first by inducing multiparametric stress, and then by releasing stress and promoting growth of the surviving cells.

With this in mind, we have studied the genomic surveillance mechanisms reflected by growth, ploidy, sensitivity to apoptosis, and p53 transactivation during the establishment of NIH 3T3 cells that express core constitutively, and finalised this with *in vivo* assessment of their tumorigenic potential.

2. Materials and methods

2.1. Plasmids

Plasmid pCMVcore191 carrying gene for HCV core aa 1-191 (**AF176573**) under the control of CMV IE promoter was described earlier [18]. Neomycin-resistance gene (*Neo*^{r}) was amplified from pRC-CMV (Invitrogene, Carlsbad, CA) and inserted into pCMVcore191 to generate pCMVcore191Neo^r. Plasmid pCMVNS3Neo^r encoding ATPase/helicase (NS3) of HCV 274933RU and *Neo*^{r} was constructed likewisely from pCMVNS3 described previously [19]. Control pCMVNeo^r was a pUC8-based vector with the Neo^r-coding cassette, and CMV IE promoter. Plasmid pCMVcore152 encoding C-terminus truncated version of HCV core aa 1-152 was described earlier [18]. Reporter plasmid pG13-luc carrying 13 repeats of the consensus wild-type p53 binding sequence was kindly provided by Dr WS El-Deiry [11]. Plasmid pSVβ-gal expressing β-galactosidase was purchased (Promega, Madison, WI).

2.2. Cells

NIH 3T3 was maintained in DMEM (Life Technologies, Inc., Gaithersburg, MD) supplemented with 10% fetal calf serum (FCS; Life Technologies). To avoid spontaneous transformation, cells were not allowed to reach confluency, and were re-plated 1 : 5 every three days. Cells were transfected/co-transfected with plasmids using LipofectAMINE^{TM} (Life Technologies), and in transient transfections, harvested after 48 h. To create cell lines of NIH191 series, NIH 3T3 were transfected with pCMVcore191Neo^r; and for NIHNS series, with pCMVNSNeo^r. Control NIH 3T3 cells were transfected with pCMVNeo^r alone. Clones were selected on G418-containing medium (40 μg/ml) as was described [52].

2.3. Mice

Female, 10 weeks old, C.B-17/SCID mice [2] were bred under pathogen-free conditions and maintained at the animal facility of the Swedish Institute for Infectious Disease Control, Sweden.

2.4. Immune stainings

Western blotting was done with primary anti-HCV core- [18] or NS3- [19] antibodies, peroxidase-conjugated secondary antibodies (DAKOPatts AB, Copenhagen, Denmark) using chemiluminiscence detection system (ECL kit; Amersham-Pharmacia Biotech, Piscataway, NJ) as was described [18,19].

2.5. Cell proliferation assays

To determine the doubling time, cells were seeded in 35 mm dishes at a density of 2×10^4 cells/dish. Cells were fed DMEM with 10% FCS every day, the number of cells from duplicate plates were counted manually with a hemocytometer every other day. The doubling time was determined from the growth curve. The saturation density was determined as the number of cells at confluence divided by the dish area. To estimate plating efficiencies, 200–400 cells were seeded in 50-mm dishes containing 10 ml of DMEM supplemented with 10% FCS. Cells formed colonies within 2 weeks, plates were then stained with 0.1% Crystal Violet in 25% ethanol. Colonies with more than 50 cells were scored.

2.6. Anchorage-independent growth assay

Soft agar dishes (50 mm) were prepared with an underlayer of 0.5% agar (Difco, Detroit, MI, USA) in DMEM containing 10% FCS. Cells were seeded in the dishes in DMEM containing 10% FCS and 0.33% agar at a density of 4×10^3 cells/dish. Colonies that developed in the agar suspension 2 weeks after seeding, were counted and photographed using phase-contrast photomicrography; those with $>$200 cells ($\geqslant$0.1 mm in diameter) were scored. Results were expressed as % of colonies formed per total number of seeded cells. Each experiment was performed in triplicate.

2.7. Flow cytometry

Cells were harvested, washed in PBS, permeabilized with 0.1% saponin for 0.5 h, washed in PBS, stained with a solution containing propidium iodide (50 μg/ml) and RNase (2 U/ml), and analysed on ODAM ATC-3000 flow sorter-analyser (Bruker Spectrospin, Wissembourg, France) by one-parameter FACScanning. The analysis rate was 400–600 cells/sec. A total of 15 000–20 000 cells were analysed in each sample. For serum starvation, cells in exponential growth phase (60–80% confluence) were rinsed with PBS, and cultured in DMEM with 0.5% FCS for up to 9 days. For G2/M arrest, cells at 70% confluence were treated with nocodazole (200 ng/ml; Sigma) for 24 h. Ploidy was assessed using diploid mouse splenocytes as an internal standard. Clones were assessed in three independent runs. Data was processed using ModFit 2.0 software (Verity Software House Inc., Topsham, ME).

2.8. Reporter gene assays

NIH 3T3 were co-transfected with reporter plasmids pG13-luc and pSVβ-gal, or with reporter plasmids and either pCMVcore191, or pCMVcore152. NIH191 cell lines were co-transfected with pG13-luc and pSVβ-gal. After 48 h, cells were lysed with Luciferase Cell Culture Lysis Buffer (Promega, Madison, WI). Soluble proteins were recovered and quantified using Bradford assay (BioRad, Hercules, CA). Luciferase activity in soluble fractions was measured using Luciferase Assay System (Promega), and β-galactosidase activity, using ortho-nitrophenyl-galactopyranoside (4 mg/ml; Sigma). The p53-dependent transactivation was represented as a mean ratio of luciferase to β-galactosidase activity in three independent experiments.

2.9. Tumorigenicity

NIH191-3, NIH191-10, or NIHNS clones were cultured to 70% confluency, harvested using 0.001% trypsin and 0.02% EDTA for 5 min at 37°C, washed once in DMEM with 2% FCS and once with PBS, and re-suspended in PBS. Age-matched groups of C.B-17/SCID mice (3–4/group) were inoculated subcutaneously in the abdomen with 2×10^4, or 2×10^5, or 2×10^6 of NIH191-3, or NIH191-10, or NIHNS cells suspended in 100 μl PBS, or sham-inoculated with PBS. Tumors were monitored by palpating at 2-day intervals, and measured with the Vernier calipers. When first tumors reached 10 mm in diameter, all mice were anethized, and sacrificed. Tumors were removed and evaluated as was described [26]. Half of each of the excised tumors was frozen at -70°C, and half was formalin-fixed and paraffin-imbedded. Frozen tissues and paraffin blocks were cut into 7–9 μm sections, and fixed. Paraffin sections were routinely stained with hematoxylin and eosin (H&E). Frozen sections were stained with anti-HCV core [18], or control antibodies as was described earlier [43].

3. Results

3.1. HCV core-gene expression in NIH 3T3 transfectants

We established cell lines that expressed HCV core constitutively as judged by specific immunofluorescence staining and Western blot done using previously described core-specific rabbit polyclonal serum [18] (Fig. 1). Western blotting demonstrated expression of proteins with the molecular mass of approximately 21 and 19 kDa (Fig. 1C), the shorter form appearing as a result of the earlier shown processing of the full-length HCV core [29,39]. Immunofluorescence analysis revealed strong perinuclear granular staining and a weaker nuclear staining (Fig. 1A,B). Double staining was consistent with the coexistence of two forms, the full length localizing in the cytoplasm, and the processed localizing in the nucleus [32]. Core-specific rabbit serum did not stain the control HCV NS3-expressing NIH 3T3 cell line, and NIH191-3 and NIH191-10 cells were not stained with sera collected from the rabbit prior to core immunization (data not shown).

3.2. Growth properties and morphology of HCV core gene-transfected NIH 3T3

Phenotypic changes in the HCV core gene-transfected cells were observed already at the early passages. Transfected cells had numerous flattened giant cells (but no multinucleated giant cells), and did not reach confluency even after one week. Expression of core protein led to an increase in the mean doubling time and a decrease in the saturation density (Table 1). Colony formation efficiency assays demonstrated a substantial reduction in the number of colonies as compared to the control NIH 3T3 and NIH 3T3 *Neo*^{r} cells (Table 1). After approximately 50 passages, the phenotype of the surviving clones (c.a. 30%) has changed. Giant cells disappeared. Doubling time decreased, while saturation density and colony formation efficiency were restored to the NIH 3T3 levels (Table 1). Simultaneously, cells acquired focus-forming morphology (data not shown). Clones formed significant numbers of colonies in soft-agar medium, strongly indicating the transformed phenotype (Fig. 2). These characteristics were retained even after re-populations at low density done to eliminate core expressing, but non-transformed sub-clones. No morphological changes were observed in the iden-

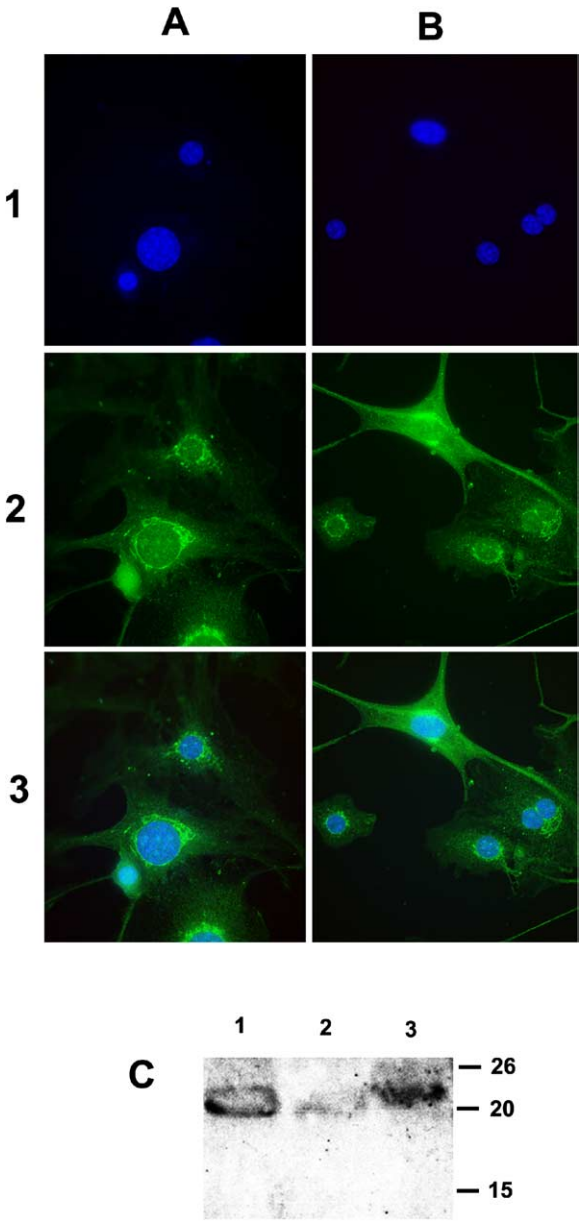

Fig. 1. Analysis of stable NIH 3T3 clones expressing HCV core after 100 passages. Immunofluorescence staining of NIH191-3 (panel A); and NIH191-10 (panel B), clones. Fields 1–2 in each of the panels visualize one area recorded after excitation with ultraviolet light for nuclear staining (field 1); with 488 nm light for FITC staining (field 2); overlay of fields 1 and 2 (field 3). Panel C illustrates Western blotting of stable clones NIH191-10 (lane 1), NIH191-3 (lane 2), and NIH 3T3 transiently transfected with the plasmid expressing full-length HCV core pCMVcore191 (lane 3). On the right are positions of 14.9, 19.6 and 26 kDa molecular mass markers.

Table 1
Growth properties of murine fibroblasts NIH 3T3 stably transfected with Neo^r and HCV core gene, as compared to parental NIH 3T3

Growth properties	NIH 3T3	NIH 3T3 constitutively expressing hepatitis C virus core			
		Preneoplastic stage		Neoplastic stage	
		191/3	191/10	191/3	191/10
Doubling time, h	22	33	29	24	24
Saturation density, cells/cm^2 $\times$ 10^4	44 ± 3	18 ± 4	25 ± 2	40 ± 4	78 ± 3
Plating efficiency, %	7.8 ± 1.1	1.75 ± 0.3	2.05 ± 0.6	4.8 ± 0.3	8.9 ± 0.3
Growth in soft-agar medium, %	0	0	0	3.3	6.9

Note. Points are means of at least three independent experiments; errors are the standard errors of the mean (SEM).

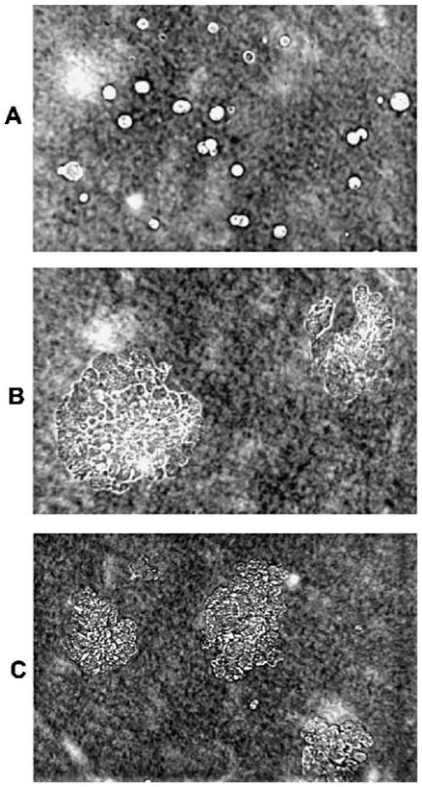

Fig. 2. Colony formation in soft-agar medium by NIH 3T3 Neo^r (A), and clones constitutively expressing HCV core NIH191-3 (B), and NIH191-10 (C).

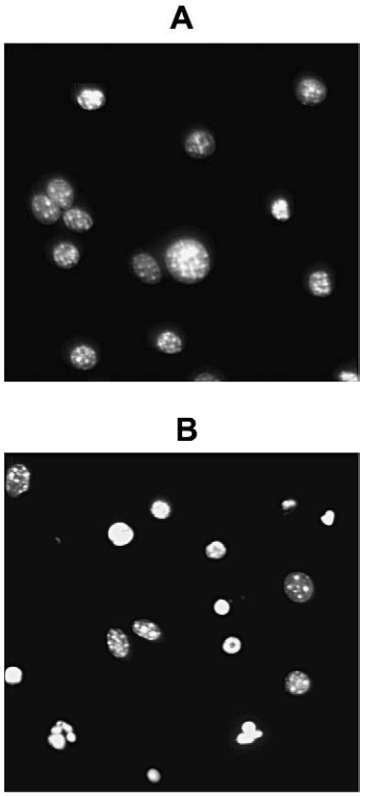

Fig. 3. Cell survival after 4 days of serum starvation, HCV core-expressing clone NIH191-3 (A), and control NIH 3T3 Neo^r (B).

tically treated NIH3T3 cells transfected with Neo^r-vector alone. Two typical clones, one with a lower, and one with a higher level of core expression, designated NIH191-3 and NIH191-10 (Fig. 1) were taken into a further study.

3.3. *Suppression of serum starvation-induced cell death*

We next analysed the effect of stable core expression on the sensitivity of cells to apoptosis induced by serum starvation. In concordance with the data for the *in vitro* cultured skin fibroblasts [65], cells starved for 1 day showed no significant increase in apoptosis (data not shown). After 3–4 days of starvation, NIH 3T3 Neo^r clones began to die exhibiting extensive cell rounding, shrinkage, cytoplasmic blabbing, and chromatin condensation, while core-expressing cells remained alive (Fig. 3). After 6 days, the percentage of apoptotic cells with fragmented/apoptotic DNA ($<$2N) was 31% in NIH 3T3 Neo^r, 2.5% in NIH191-3, and 7% in NIH191-10 clones (Fig. 2).

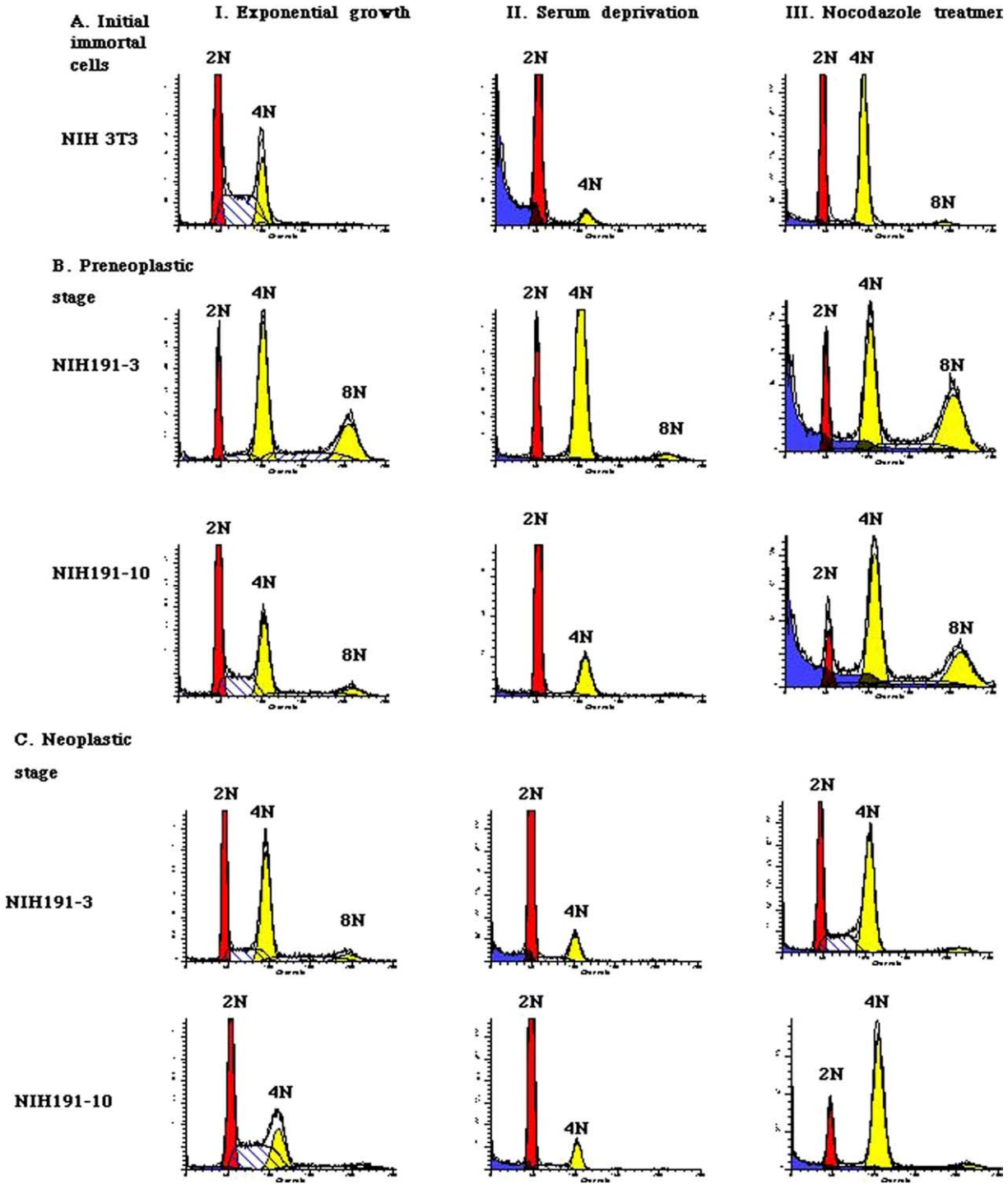

Fig. 4. Flow cytometry cell cycle analysis of NIH 3T3 (A), NIH191-3 and NIH191-10 cells at preneoplastic stage (B), and NIH191-3 and NIH191-10 cells at neoplastic stage (C). Panel I, cells growing exponentially; panel II, 6 days of serum starvation; panel III, 48 h of nocodazole treatment. X-axis, DNA content, Y-axis, number of cells. NIH 3T3 is an aneuploid cell line, but for convenience is called "diploid". Diploid NIH 3T3 cells in G0/G1 are marked 2N (red colour), diploid G2/M and tetraploid G0/G1 cells are indicated as 4N, tetraploid NIH 3T3 cells in G2/M are indicated as 8N (yellow). DNA content between 2N and 4N corresponds to the diploid S-phase cells, and between 4N and 8N, to tetraploid S-phase cells.

Table 2
Spindle assembly check-point function in NIH 3T3 and HCV core-expressing NIH 3T3 Neo^r-based stable cell lines

Cell line	% cells endoreduplicating, untreated cells	% cells endoreduplicating, nocodazole-treated cells
NIH 3T3	<2	4
NIH191-3		
preneoplastic stage	37	45
neoplastic stage	14	6
NIH191-10		
preneoplastic stage	11	37
neoplastic stage	5	8

Comment: Cells were incubated for 48 h with or without nocodazole, harvested and treated as described in Materials and methods. The fraction of cells with DNA content >4N in S, G2 and M compartments was determined as a measure of endoredupication. Defective spindle assembly checkpoint function was recognized by the significantly increased percentage of nocodazole-treated cells that underwent endoreduplication.

3.4. Activity of mitotic spindle cell cycle checkpoint

The activity of the mitotic spindle cell cycle checkpoint during transformation was analysed by flow cytometry. At the preneoplastic stage, FACS analysis of NIH191-3 and NIH191-10 clones revealed three peaks with DNA content 2N, 4N and 8N; all cells with DNA content of over 4N were accounted for as "tetraploids" (Fig. 4, panel I). Since G2/M diploids and G0/G1 tetraploids cannot be distinguished (both 4N), we synchronised both in the G0/G1 phase by serum deprivation, and thus estimated maximal possible amount of tetraploid cells (Table 2). This value is overestimated due to counting in diploid cells in the G2/M phase. Nocodazole arrests both suspension and adherent cells in the metaphase preventing spindle formation. By nocodozole-induced G2/M arrest, we estimated minimal amount of tetraploids and then compared both populations.

In NIH191-3 at both preneoplastic and neoplastic stages, the amounts of tetraploids estimated by serum starvation and nocodazole treatment were concordant, although at preneoplastic stage, % of cells with DNA population >4N was higher than >4N DNA population estimated by serum deprivation (Table 2). In NIH191-10 at preneoplastic stage, on contrary, the minimal possible amount of tetraploids determined by the nocodazole treatment grossly exceeded maximal determined by serum starvation (Table 2; Fig. 4, panels II, III). It implies that at the preneoplastic stage, some NIH191-3 and at least 20% of NIH191-10 cells became polyploid by proceeding through new rounds of DNA synthesis without completing mitosis.

A period of genomic instability ended by formation of aneuploids with a normal diploid cell cycle. Tetraploid cells were significantly reduced in both clones; in the NIH191-10 clone they practically disappeared (Fig. 4C). Chromosome instability and loss was reflected by the change in the DNA index from 1.67 for parental NIH 3T3 to 1.58 for both NIH191-3 and NIH191-10.

3.5. Tumorigenicity

Next, we evaluated the tumorigenic potential of stable HCV-core expressing NIH 3T3 cells in SCID mice using as a control malignant NIH 3T3 transformed by stable expression of HCV NS3 (as was described [52]; NIHNS). IF staining and Western blot of the cells after a large scale culture done for to the mouse challenge, confirmed that NIH191-3 and 191-10 stably expressed HCV core, albeit at different levels (Fig. 1C, lanes 1 and 2).

When inoculated into SCID mice, core-expressing NIH 3T3 clones rapidly generated solid tumors (Fig. 5). NIH191-10 grew exponentially in all recipients of the high dose (100%) and in 75% recipients of the medium dose with a latency of 5 days (Fig. 5). NIH191-3 inoculated at medium and high cell dose showed limited growth in totally 33% mice (Fig. 5). Tumors appeared with the latency of 5 days and stopped growing by day 7 (Fig. 5). NIHNS cells inoculated at medium and high dose demonstrated limited growth palpable as soft pads in all mice. They appeared by day 4, but started to recede by day 7 (Fig. 5). Excised sites of inoculation of NIHNS cells were found to contain encapsulated cell suspensions, but no solid tumors. All in-

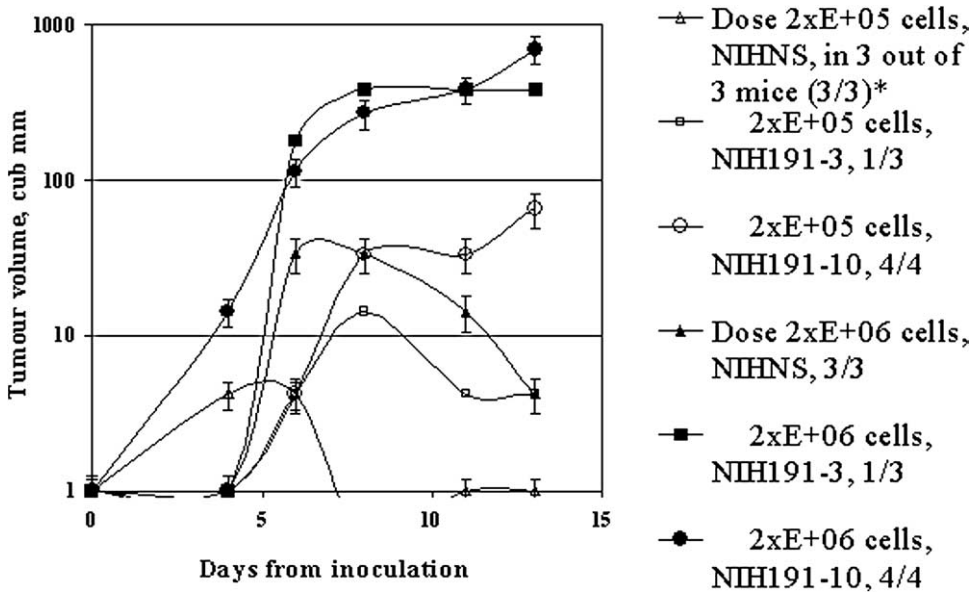

Fig. 5. Tumorigenicity of NIH 3T3-derived stable cell lines expressing HCV core (NIH191-3, NIH191-10), and a control cell line with a low-level expression of HCV NS3 protein (NIHNS), after inoculation into C.B-17/SCID mice. *Number of mice with palpable solid or soft tumors per total number of inoculates.

oculations of NIHNS, NIH191-3, and NIH191-10 cells done at a low dose (2×10^4 cells) were rejected. No tumors were observed in mice sham-inoculated with PBS or with up to 2×10^6 of the human colonic epithelium cells (J. Hinkula, unpublished). Macroscopic examination of mice revealed no metastases.

NIH191-3 and NIH191-10-derived solid tumors consisted of collagen fiber fascicles interlaced in different directions, with connective elements to fibroblasts and fibrocytes (Fig. 6A,B). The majority of cells had a spherical shape. Cell nuclei were polymorphic in size, form, and level of heterochromatization (Fig. 6). Cell polymorphism, increased prominent nucleoli and numerous scattered mitotic figures indicated a sarcomatous process. Some tumor areas were marked with dystrophic changes of cells (nuclear pyknosis, karyorrhexis, karyolysis). In these areas, the connective tissue component prevailed over the cellular one. Tumor outgrowths had numerous dilated capillaries, and in some areas, the sinusoid type vessels. The overall microscopic appearance indicated formation of spindle cell sarcomas (see www.usc.edu/hsc/dental/PTHL501/SA/csa27.html). Tumors were stained by core-specific rabbit serum demonstrating that after inoculation into mice, cells continued to express HCV core (Fig. 7A–C). This serum did not stain the area of encapsidation containing a suspension of NS3-expressing NIHNS (Fig. 7D). Tumors induced by NIH191-3 and NIH191-10 were not stained by the preimmune rabbit serum (Fig. 7E, and data not shown).

3.6. Influence of HCV core on the p53 transactivation

Genetic instability, resistance to apoptosis and tumorigenicity pointed at possible p53 dysfunction. To examine this, we investigated stored NIH191-3 and NIH191-10 clones that were used for tumor induction, for the status of the endogenous p53 transactivation. NIH 3T3 carries transcriptionally active wild-type p53 gene [16,61]. Similarity between human and murine p53 and p53 responsive elements [50] permitted monitoring using the consensus p53 response element [11]. The p53 transactivation in NIH191-3 and NIH191-10 clones was decreased 5- to 10-fold (Fig. 8). Similar effect was observed after transient transfection of the parental NIH 3T3 by a plasmid encoding amino acids 1 to 152 of HCV core. At the same time, transient expression of the full-length HCV core induced an increase in the endogenous p53 transactivation (Fig. 8).

4. Discussion

The transforming ability of HCV core protein was so far considered as rather weak. It was tumorigenic in combinations with proto-oncogenes, or over-expressed

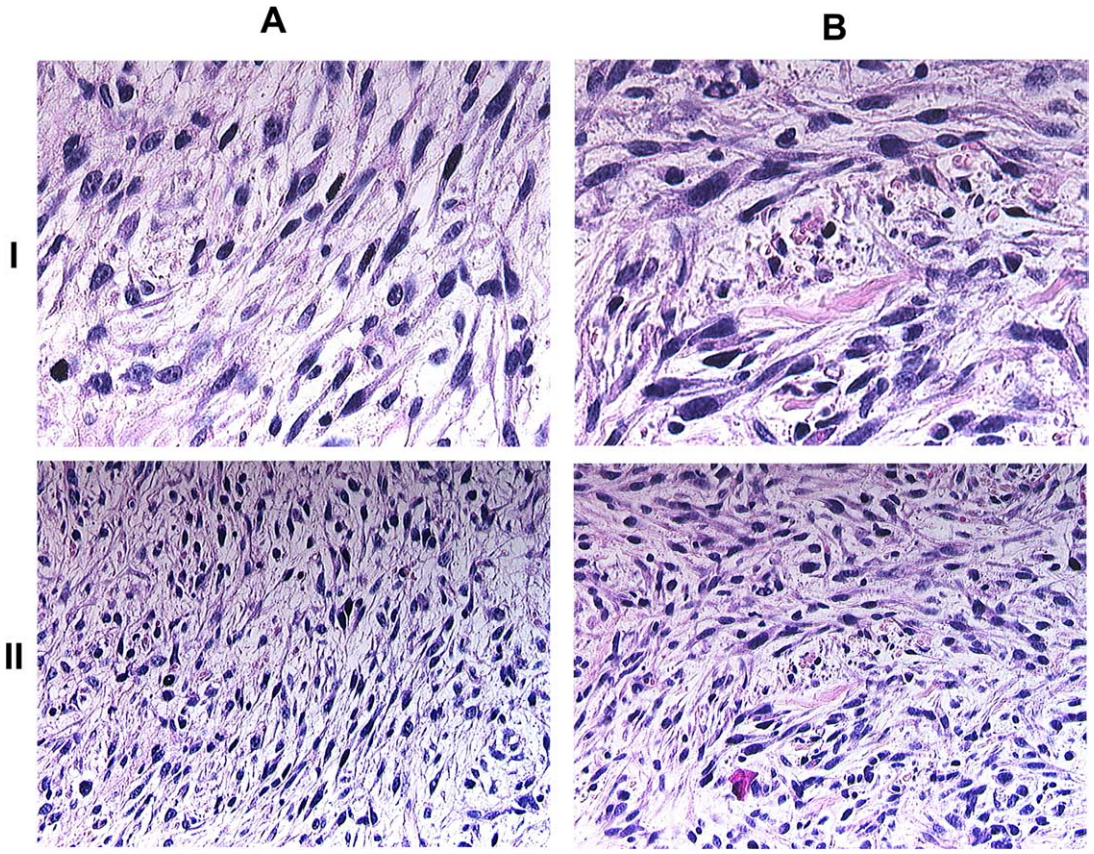

Fig. 6. Hematoxylin & Eosin staining of formaldehyde-fixed paraffin-imbedded sections of solid tumors formed by NIH191-10 (A, mouse no. 1; B, mouse no. 4). Field I, magnification ×40; field II, ×20.

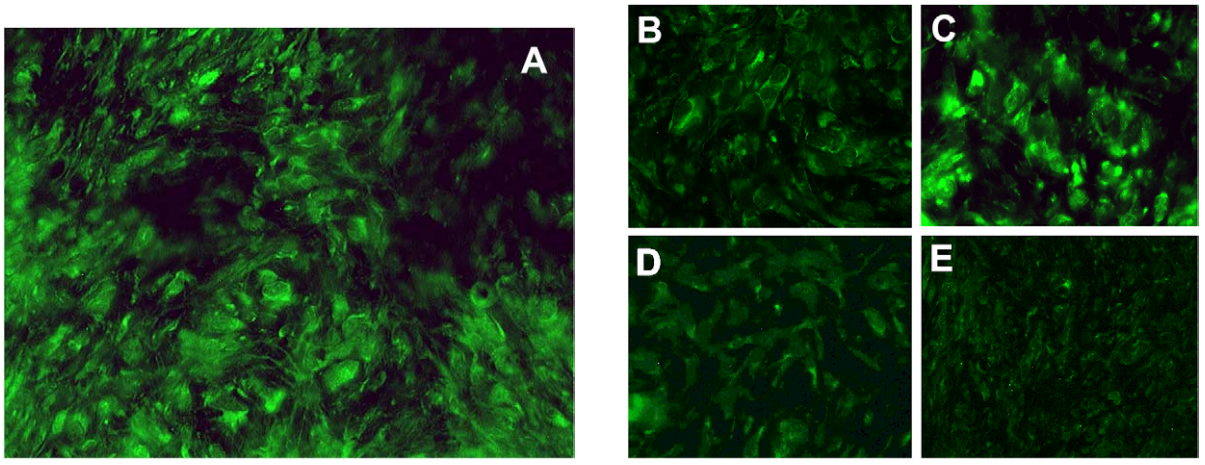

Fig. 7. Frozen sections of solid tumors induced by NIH191-3 at magnifications ×20 (A), and ×40 (B), and by NIH191-10 at magnification ×40 (C), sections stained with core-specific polyclonal rabbit serum 34-6. Area of incapsidation containing suspension of control NIHNS cells stained with anti-core rabbit serum 34-6 at magnification ×40 (D). Solid tumor induced by NIH191-10 stained with the preimmune rabbit serum 34-0 at magnification ×20 (E).

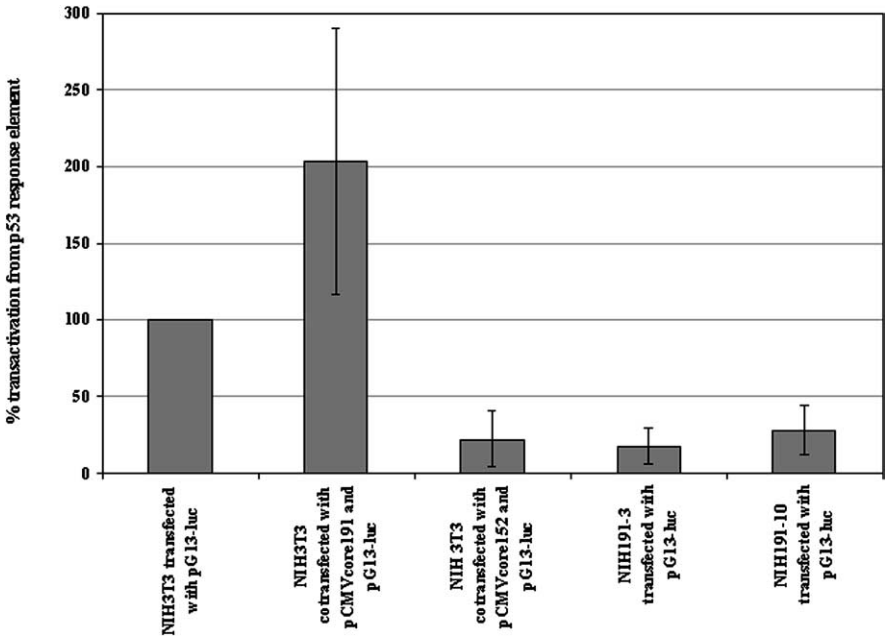

Fig. 8. Transcriptional activation of p53 in the HCV core-expressing clones NIH191-3, and NIH191-10 as compared to the parental NIH 3T3 taken for 100%. To estimate the influence of HCV core on the endogenous p53, NIH191-3 and NIH191-10 were transfected with luciferase-expressing reporter plasmid pG13-luc, and parental NIH 3T3 were co-transfected with pG13-luc and pCMVcore191, or pCMVcore152.

cell cycle regulating proteins [59,64], but until recently was thought to be unable to completely transform cells and induce tumors [4,21,44]. Here, typical NIH 3T3 clones adapted for growth in the presence of HCV core were selected, and followed up longitudinally. We scrutinised cell physiology (growth, ploidy, sensitivity to apoptosis) during the establishment of NIH 3T3 that expressed HCV core constitutively, to see whether HCV core alone could promote cells to become cancerous.

During the establishment stage [34], HCV core activity was first seen as the inhibition of NIH 3T3 cell growth. We have shown that the inhibition of cell growth by HCV core was accompanied by genomic instability. The earliest change in the cell ploidy was the appearance of tetraploid ($\geqslant$4N) cells. While in the NIH191-3 clone, the tetraploid cells consisted of diploid ($\geqslant$2N) and tetraploid ($\geqslant$4N) subpopulations, in the NIH191-10 clone, the tetraploids appeared from the diploid cells as a result of the disrupted mitotic checkpoint. In the rat embryo fibroblast model of multistep oncogenesis, polyploidy serves as the initiator of neoplasm/tumor growth as the polyploid cells have an advantage over diploids in more efficient utilization of resources (albeit slow growth) [5].

The ploidy shift was abrogated by genetic aberrations that accumulate during prolonged selection [13]. Indeed, in the core-expressing NIH 3T3 at the stabilization stage, the tetraploids underwent a period of chromosome instability and DNA loss leading to a decreased DNA index identical for NIH191-3 and NIH191-10. Simultaneously with DNA loss, HCV core expressing NIH 3T3 clones acquired anchorage independence and absence of contact inhibition, the essential alterations determining malignancy [13]. The neoplastic/promotion stage of HCV core-induced transformation was characterized by yet another marker of malignant transformation – the suppression of apoptosis, observed also in the earlier studies [42,45,56]. In NIH191-10 clone with higher level of HCV core expression, genomic instability was attained through the disruption of mitotic spindle cell checkpoint, other mechanisms could be active in the NIH191-3 clone that expressed HCV core at a lower level. Interestingly, the effects of HCV core on the cell viability and p53-dependent transcription were also found to be concentration dependent [23,42,48].

A pivotal genetic event in the loss of the control over the genomic instability and hepatocellular carcinogenesis is the p53 dysfunction [49,60]. In concordance with the previously published data [46], NIH 3T3 transformed by HCV core expression exhibited a 5- to 10-fold reduced p53 transactivation ability. This could have directly or indirectly promoted the neoplas-

tic transformation. Inhibition of p53 transactivation in NIH 3T3 expressing core constitutively (and thus harbouring the processed C-terminus deleted HCV core [29,39]) was mimicked by transient transfection into NIH 3T3 of the gene encoding HCV core amino acids 1 to 152. Full-length unprocessed HCV core provided by transient transfection induced an increase in p53 transactivation (that may have been attained through transient core-induced increase in p53 expression [55]). As it was recently demonstrated, HCV core targets the p53 pathway via three routes: physical interaction, post-translational p53 modification, and modulation of regulatory activity of p53 [23]. Notably, core can inhibit the p53-mediated apoptosis by blocking the interaction between p53 and ASPP2, a splicing version of Bcl2-binding protein that enhances the p53-induced apoptosis [3]. It can also rescue the p53-mediated suppression in both RNA polymerase I and III systems [23]. Core-induced reduction of p53 transactivation and its ability to relieve the p53-mediated suppression contribute to the loss of the control over the genomic instability and are consistent with the role of core in HCV-associated oncogenesis.

We finally evaluated the capacity of transformed NIH3T3 expressing HCV core to form solid tumors in the immunocompromised host. In SCID mice, syngenic cells/tumor cell lines/tumors are grafted with an average latency of 25 days (for C.B-17/SCID mice; [12]), while allogenic grafts and tumors are rejected by the NK cells [35]. Numerous previous experiments have shown NIH 3T3 and NIH 3T3-derived Neo^r-transfectants to be non-tumorigenic (see, for example, [25,52,57]). Allogenic NS3-expressing NIHNS used here as a tumor-control were, on contrary, expected to induce tumors [52]. However, high-dose inoculates of NIHNS did not form solid tumors. The latter together with the rejection of all cell inoculates at a low dose, indicated potent NK cell activity. Despite this, cells expressing high levels of HCV core that underwent the mitotic spindle cell checkpoint disruption induced solid tumors in 88% of the recipients in only five days. The low-level core expressing cell line that at preneoplastic stage had basically kept undisrupted mitotic spindle cell check-point was weakly tumorigenic. Thus, constitutive HCV core expression turned NIH 3T3 into malignant cells.

Recently, constitutive expression of core was shown to completely transform the Chang-liver cells [53]. Transformation was registered by changes in cell morphology, increased proliferation rate seen as an increased proportion of cells in the S-phase, and varying DNA content. Injected into nude mice, core-transformed Chang-liver cells induced tumors that were morphologically typed as hepatocarcinomas [53]. Here, we made a step further describing both the events preceding and concomitant with transformation (preneoplastic and neoplastic stages), detailed changes in the DNA content as the increased ploidy followed by DNA loss, and depicted the disruption of the mitotic spindle cell checkpoint as the start-off of the transformation. Altogether, these data prove that HCV core alone is sufficient to induce malignant transformation of various cell types, and indicate that the pathway of this transformation seem to be shaped by the HCV core dose (expression level). Our results demonstrate that HCV core, with an accent on its processed form, acts by inducing first stress, and then stress release and unconditioned growth of core-expressing survivor cells through promotion of genomic instability and violation of the cell cycle checkpoints.

Core proteins derived from the tumor tissues possess multiple mutations and deletions [9,15,40,51] and possibly different biological properties [9]. There are other indications that core variants differ in their effects on cellular signaling [9,47]. For example, core of HCV 1b activated [8,36,63], while core of HCV 1a suppressed nuclear factor kappaB (NF-κB) signaling [22,47,54] with differential regulation attributed to single amino acid polymorphisms [47]. HCV 1b core gene used here (**AF176573**) harbours some of the mutations associated with HCC, as G instead of S in position 45 [15], and V in place of A at position 147 [40], and aligns well with core sequences isolated from hepatocellular carcinomas (**AB077722**, **AB077725**, **AB077728**, **AB077739**, **AB077743**; [40]). Also, it has crucial amino acids R9 and K11 involved in the activation of NF-κB signaling and consequent inhibition of apoptosis [47]. These may have contributed to the carcinogenicity of our HCV core variant. However, one should keep in mind that the capacity to interfere with cellular signalling had been repeatedly assigned to a multitude of core variants. Core of genotypes 1b, 2a, and 4d were shown to induce similar changes in the expression of genes involved in metabolism, signal transduction, protease activity, immune responses, and apoptosis [10]. We had completely transformed fibroblast cell line by constitutive expression of core of HCV 1b, while Shan Y. et al. achieved it by constitutive expression of core of HCV 2b [53]. Mice transgenic for HCV 1a core, E1 and E2 were also prone to liver and lymphoid tumor development [38]. Altogether, this indicates a basic role of HCV core in establishment and maintenance of neoplastic transformation.

We speculate here that versatile effects of HCV core on the host cells reflect general property of HCV core protein, and depend more on the levels of expression achieved, site of protein localization in the cell, cell type utilized, and the cellular environment than on a specific core sequence. This capacity of HCV core to induce cell re-programming is one of the tools used by hepatitis C virus for survival and propagation.

Acknowledgements

This work was funded by the grants of the New Visby programme of the Swedish Institute, EU grants ERB IC CT98-0313 and 05-1000004-7748 to Maria Isaguliants, and Swedish Research Council grant to Jorma Hinkula. Drs Karl Ljungberg, Galina Selivanova, David M. Goldenberg, and Anna Kuznetzova are gratefully acknowledged for valuable comments and criticisms.

References

[1] H. Aoki, J. Hayashi, M. Moriyama, Y. Arakawa and O. Hino, Hepatitis C virus core protein interacts with 14-3-3 protein and activates the kinase Raf-1, *J. Virol.* **74** (2000), 1736–1741.

[2] G.C. Bosma, R.P. Custer and M.J. Bosma, A severe combined immunodeficiency mutation in the mouse, *Nature* **301** (1983), 527–530.

[3] Y. Cao, T. Hamada, T. Matsui, T. Date and K. Iwabuchi, Hepatitis C virus core protein interacts with p53-binding protein, 53BP2/Bbp/ASPP2, and inhibits p53-mediated apoptosis, *Biochem. Biophys. Res. Commun.* **315** (2004), 788–795.

[4] J. Chang, S.H. Yang, Y.G. Cho, S.B. Hwang, Y.S. Hahn and Y.C. Sung, Hepatitis C virus core from two different genotypes has an oncogenic potential but is not sufficient for transforming primary rat embryo fibroblasts in cooperation with the H-ras oncogene, *J. Virol.* **72** (1998), 3060–3065.

[5] N. Chikatsu, Y. Nakamura, H. Sato, T. Fujita, S. Asano, and T. Motokura, p53 mutations and tetraploids under r- and K-selection, *Oncogene* **21** (2002), 3043–3049.

[6] J.W. Cho, W. Baek, S.I. Suh, S. Yang, J. Chang, Y.C. Sung and M.H. Suh, Hepatitis C virus core protein promotes cell proliferation through the upregulation of cyclin E expression levels, *Liver* **21** (2001), 137–142.

[7] J.W. Cho, W. Baek, S. Yang, J. Chang, Y.C. Sung and M.H. Suh, HCV core protein modulates Rb pathway through pRb down-regulation and E2F-1 up-regulation, *Biochim. Biophys. Acta* **1538** (2001), 59–66.

[8] Y.M. Chung, K.J. Park, S.Y. Choi, S.B. Hwang and S.Y. Lee, Hepatitis C virus core protein potentiates TNF-alpha-induced NF-kappaB activation through TRAF2-IKKbeta-dependent pathway, *Biochem. Biophys. Res. Commun.* **284** (2001), 15–19.

[9] N. Delhem, A. Sabile, R. Gajardo, P. Podevin, A. Abadie, M.A. Blaton, D. Kremsdorf, L. Beretta and C. Brechot, Activation of the interferon-inducible protein kinase PKR by hepatocellular carcinoma derived-hepatitis C virus core protein, *Oncogene* **20** (2001), 5836–5845.

[10] J. Dou, P. Liu and X. Zhang, Cellular response to gene expression profiles of different hepatitis C virus core proteins in the Huh-7 cell line with microarray analysis, *J. Nanosci. Nanotechnol.* **5** (2005), 1230–1235.

[11] W.S. el-Deiry, T. Tokino, V.E. Velculescu, D.B. Levy, R. Parsons, J.M. Trent, D. Lin, W.E. Mercer, K.W. Kinzler and B. Vogelstein, WAF1, a potential mediator of p53 tumor suppression, *Cell* **75** (1993), 817–825.

[12] A.M. Engel, I.M. Svane, J. Rygaard and O. Werdelin, MCA sarcomas induced in scid mice are more immunogenic than MCA sarcomas induced in congenic, immunocompetent mice, *Scand. J. Immunol.* **45** (1997), 463–470.

[13] D. Hanahan and R.A. Weinberg, The hallmarks of cancer, *Cell* **100** (2000), 57–70.

[14] J.H. Hoofnagle, Course and outcome of hepatitis C, *Hepatology* **36** (2002), S21–29.

[15] C. Horie, H. Iwahana, T. Horie, I. Shimizu, K. Yoshimoto, S. Yogita, S. Tashiro, S. Ito and M. Itakura, Detection of different quasispecies of hepatitis C virus core region in cancerous and noncancerous lesions, *Biochem. Biophys. Res. Commun.* **218** (1996), 674–681.

[16] T.S. Huang, M.L. Kuo, J.Y. Shew, Y.W. Chou and W.K. Yang, Distinct p53-mediated G1/S checkpoint responses in two NIH3T3 subclone cells following treatment with DNA-damaging agents, *Oncogene* **13** (1996), 625–632.

[17] R. Idilman, N. De Maria, A. Colantoni and D.H. Van Thiel, Pathogenesis of hepatitis B and C-induced hepatocellular carcinoma, *J. Viral Hepat.* **5** (1998), 285–299.

[18] M.G. Isaguliants, N.V. Petrakova, E.V. Kashuba, Y.G. Suzdaltzeva, S.V. Belikov, V.V. Mokhonov, A.G. Prilipov, L. Matskova, I.S. Smirnova, C. Jolivet-Reynaud and E. Nordenfelt, Immunization with hepatitis C virus core gene triggers potent T-cell response, but affects CD4+ T-cells, *Vaccine* **22** (2004), 1656–1665.

[19] M.G. Isaguliants, N.V. Petrakova, V.V. Mokhonov, K. Pokrovskaya, Y.G. Suzdaltzeva, A.V. Krivonos, A.D. Zaberezhny, M.M. Garaev, V.D. Smirnov and E. Nordenfelt, DNA immunization efficiently targets conserved functional domains of protease and ATPase/helicase of nonstructural 3 protein (NS3), of human hepatitis C virus, *Immunol. Lett.* **88** (2003), 1–13.

[20] T. Ishikawa, K. Shibuya, K. Yasui, K. Mitamura and S. Ueda, Expression of hepatitis C virus core protein associated with malignant lymphoma in transgenic mice, *Comp. Immunol. Microbiol. Infect. Dis.* **26** (2003), 115–124.

[21] D.Y. Jin, H.L. Wang, Y. Zhou, A.C. Chun, K.V. Kibler, Y.D. Hou, H. Kung and K.T. Jeang, Hepatitis C virus core protein-induced loss of LZIP function correlates with cellular transformation, *EMBO J.* **19** (2000), 729–740.

[22] M. Joo, Y.S. Hahn, M. Kwon, R.T. Sadikot, T.S. Blackwell and J.W. Christman, Hepatitis C virus core protein suppresses NF-κB activation and cyclooxygenase-2 expression by direct interaction with IκB kinase beta, *J. Virol.* **79** (2005), 7648–7657.

[23] C.F. Kao, S.Y. Chen, J.Y. Chen and Y.H. Wu Lee, Modulation of p53 transcription regulatory activity and post-translational modification by hepatitis C virus core protein, *Oncogene* **23** (2004), 2472–2483.

[24] N. Kato, H. Yoshida, S. Kioko Ono-Nita, J. Kato, T. Goto, M. Otsuka, K. Lan, K. Matsushima, Y. Shiratori and M. Omata, Activation of intracellular signaling by hepatitis B and C viruses: C-viral core is the most potent signal inducer, *Hepatology* **32** (2000), 405–412.

[25] E. Katz and B.J. Carter, A mutant cell line derived from NIH/3T3 cells: two oncogenes required for in vitro transformation, *J. Natl. Cancer Inst.* **77** (1986), 909–914.

[26] N. Keshava, Tumorigenicity of morphologically distinct transformed foci induced by 3-methylcholanthrene in BALB/c-3T3 cells, *Mutat. Res.* **447** (2000), 281–286.

[27] K. Koike, K. Moriya and S. Kimura, Role of hepatitis C virus in the development of hepatocellular carcinoma: transgenic approach to viral hepatocarcinogenesis, *J. Gastroenterol. Hepatol.* **17** (2002), 394–400.

[28] J. Kountouras, C. Zavos and D. Chatzopoulos, Apoptosis in hepatitis C, *J. Viral Hepat.* **10** (2003), 335–342.

[29] H.J. Kwun and K.L. Jang, Dual effects of hepatitis C virus Core protein on the transcription of cyclin-dependent kinase inhibitor p21 gene, *J. Viral Hepat.* **10** (2003), 249–255.

[30] S. Laconi, P. Pani, S. Pillai, D. Pasciu, D.S. Sarma and E. Laconi, A growth-constrained environment drives tumor progression in vivo, *Proc. Natl. Acad. Sci. USA* **98** (2001), 7806–7811.

[31] K. Li, T. Prow, S.M. Lemon and M.R. Beard, Cellular response to conditional expression of hepatitis C virus core protein in Huh7 cultured human hepatoma cells, *Hepatology* **35** (2002), 1237–12346.

[32] Q. Liu, C. Tackney, R.A. Bhat, A.M. Prince and P. Zhang, Regulated processing of hepatitis C virus core protein is linked to subcellular localization, *J. Virol.* **71** (1997), 657–662.

[33] W. Lu, S.Y. Lo, M. Chen, K. Wu, Y.K. Fung and J.H. Ou, Activation of p53 tumor suppressor by hepatitis C virus core protein, *Virology* **264** (1999), 134–141.

[34] S.E. Mamaeva, Karyotypic evolution of cells in culture: a new concept, *Int. Rev. Cytol.* **178** (1998), 1–40.

[35] J.O. Manilay and M. Sykes, Natural killer cells and their role in graft rejection, *Curr. Opin. Immunol.* **10** (1998), 532–538.

[36] H. Marusawa, M. Hijikata, T. Chiba and K. Shimotohno, Hepatitis C virus core protein inhibits Fas- and tumor necrosis factor alpha-mediated apoptosis via NF-κB activation, *J. Virol.* **73** (1999), 4713–4720.

[37] K. Moriya, K. Nakagawa, T. Santa, Y. Shintani, H. Fujie, H. Miyoshi, T. Tsutsumi, T. Miyazawa, K. Ishibashi, T. Horie, K. Imai, T. Todoroki, S. Kimura and K. Koike, Oxidative stress in the absence of inflammation in a mouse model for hepatitis C virus-associated hepatocarcinogenesis, *Cancer Res.* **61** (2001), 4365–4370.

[38] T. Naas, M. Ghorbani, I. Alvarez-Maya, M. Lapner, R. Kothary, Y. De Repentigny, S. Gomes, L. Babiuk, A. Giulivi, C. Soare, A. Azizi and F. Diaz-Mitoma, Characterization of liver histopathology in a transgenic mouse model expressing genotype 1a hepatitis C virus core and envelope proteins 1 and 2, *J. Gen. Virol.* **86** (2005), 2185–2196.

[39] H. Nguyen, M. Mudryj, M. Guadalupe and S. Dandekar, Hepatitis C virus core protein expression leads to biphasic regulation of the p21 cdk inhibitor and modulation of hepatocyte cell cycle, *Virology* **312** (2003), 245–253.

[40] S. Ogata, M. Nagano-Fujii, Y. Ku, S. Yoon and H. Hotta, Comparative sequence analysis of the core protein and its frameshift product, the F protein, of hepatitis C virus subtype 1b strains obtained from patients with and without hepatocellular carcinoma, *J. Clin. Microbiol.* **40** (2002), 3625–3630.

[41] M. Okuda, K. Li, M.R. Beard, L.A. Showalter, F. Scholle, S.M. Lemon and S.A. Weinman, Mitochondrial injury, oxidative stress, and antioxidant gene expression are induced by hepatitis C virus core protein, *Gastroenterology* **122** (2002), 366–375.

[42] M. Otsuka, N. Kato, K. Lan, H. Yoshida, J. Kato, T. Goto, Y. Shiratori and M. Omata, Hepatitis C virus core protein enhances p53 function through augmentation of DNA binding affinity and transcriptional ability, *J. Biol. Chem.* **275** (2000), 34122–34130.

[43] W. Qian, E. Kashuba, K.P. Magnusson, K. Pokrovskaja, I. Okan, G. Klein and K.G. Wiman, Role of p53 mutation in polyomavirus-induced tumorigenesis, *J. Gen. Virol.* **78** (1997), 893–903.

[44] R.B. Ray, L.M. Lagging, K. Meyer, R. Steele and R. Ray, Transcriptional regulation of cellular and viral promoters by the hepatitis C virus core protein, *Virus Res.* **37** (1995), 209–220.

[45] R.B. Ray, K. Meyer, R. Steele, A. Shrivastava, B.B. Aggarwal and R. Ray, Inhibition of tumor necrosis factor (TNF-alpha)-mediated apoptosis by hepatitis C virus core protein, *J. Biol. Chem.* **273** (1998), 2256–2259.

[46] R.B. Ray and R. Ray, Hepatitis C virus core protein: intriguing properties and functional relevance, *FEMS Microbiol. Lett.* **202** (2001), 149–156.

[47] R.B. Ray, R. Steele, A. Basu, K. Meyer, M. Majumder, A.K. Ghosh and R. Ray, Distinct functional role of hepatitis C virus core protein on NF-κB regulation is linked to genomic variation, *Virus Res.* **87** (2002), 21–29.

[48] S. Realdon, M. Gerotto, F. Dal Pero, O. Marin, A. Granato, G. Basso, M. Muraca and A. Alberti, Proapoptotic effect of hepatitis C virus CORE protein in transiently transfected cells is enhanced by nuclear localization and is dependent on PKR activation, *J. Hepatol.* **40** (2004), 77–85.

[49] M.E. Reeves and R.P. DeMatteo, Genes and viruses in hepatobiliary neoplasia, *Semin. Surg. Oncol.* **19** (2000), 84–93.

[50] M.A. Resnick and A. Inga, Functional mutants of the sequence-specific transcription factor p53 and implications for master genes of diversity, *Proc. Natl. Acad. Sci. USA* **100** (2003), 9934–9939.

[51] B. Ruster, S. Zeuzem, V. Krump-Konvalinkova, T. Berg, S. Jonas, K. Severin and W.K. Roth, Comparative sequence analysis of the core- and NS5-region of hepatitis C virus from tumor and adjacent non-tumor tissue, *J. Med. Virol.* **63** (2001), 128–134.

[52] D. Sakamuro, T. Furukawa and T. Takegami, Hepatitis C virus nonstructural protein NS3 transforms NIH 3T3 cells, *J. Virol.* **69** (1995), 3893–3896.

[53] Y. Shan, X.G. Chen, B. Huang, A.B. Hu, D. Xiao and Z.M. Guo, Malignant transformation of the cultured human hepatocytes induced by hepatitis C virus core protein, *Liver Int.* **25** (2005), 141–147.

[54] A. Shrivastava, S.K. Manna, R. Ray and B.B. Aggarwal, Ectopic expression of hepatitis C virus core protein differentially regulates nuclear transcription factors, *J. Virol.* **72** (1998), 9722–9728.

[55] S. Siavoshian, J.D. Abraham, M.P. Kieny and C. Schuster, HCV core, NS3, NS5A and NS5B proteins modulate cell proliferation independently from p53 expression in hepatocarcinoma cell lines, *Arch. Virol.* **149** (2004), 323–336.

[56] M. Takamatsu, T. Fujita and H. Hotta, Suppression of serum starvation-induced apoptosis by hepatitis C virus core protein, *Kobe J. Med. Sci.* **47** (2001), 97–112.

[57] Y. Takihara, Y. Matsuda and J. Hara, Role of the beta isoform of 14-3-3 proteins in cellular proliferation and oncogenic transformation, *Carcinogenesis* **21** (2000), 2073–2077.

[58] T.L. Tellinghuisen and C.M. Rice, Interaction between hepatitis C virus proteins and host cell factors, *Curr. Opin. Microbiol.* **5** (2002), 419–427.

[59] K. Tsuchihara, M. Hijikata, K. Fukuda, T. Kuroki, N. Yamamoto and K. Shimotohno, Hepatitis C virus core protein regulates cell growth and signal transduction pathway transmitting growth stimuli, *Virology* **258** (1999), 100–107.

[60] B. Vogelstein, D. Lane and A.J. Levine, Surfing the p53 network, *Nature* **408** (2000), 307–310.

[61] R. Wadhwa, S. Takano, M. Robert, A. Yoshida, H. Nomura, R.R. Reddel, Y. Mitsui and S.C. Kaul, Inactivation of tumor suppressor p53 by mot-2, a hsp70 family member, *J. Biol. Chem.* **273** (1998), 29586–29591.

[62] T. Yamanaka, M. Uchida and T. Doi, Innate form of HCV core protein plays an important role in the localization and the function of HCV core protein, *Biochem. Biophys. Res. Commun.* **294** (2002), 521–527.

[63] H. Yoshida, N. Kato, Y. Shiratori, M. Otsuka, S. Maeda, J. Kato and M. Omata, Hepatitis C virus core protein activates nuclear factor kappa B-dependent signaling through tumor necrosis factor receptor-associated factor, *J. Biol. Chem.* **276** (2001), 16399–16405.

[64] T. Yoshida, T. Hanada, T. Tokuhisa, K. Kosai, M. Sata, M. Kohara and A. Yoshimur, Activation of STAT3 by the hepatitis C virus core protein leads to cellular transformation, *J. Exp. Med.* **196** (2002), 641–653.

[65] Y.S. Yu, X.S. Sun, H.N. Jiang, Y. Han, C.B. Zhao and J.H. Tan, Studies of the cell cycle of in vitro cultured skin fibroblasts in goats: work in progres, *Theriogenology* **59** (2003), 1277–1289.